Asymmetrically coupled resonators for mass sensing

S. Marquez[1], M. Alvarez[2,*], J.A. Plaza[2], L.G. Villanueva[3], C. Dominguez[2] and L.M Lechuga[1]

[1] Nanobiosensors and Bioanalytical Applications Group, Catalan Institute of Nanoscience and Nanotechnology (ICN2), CSIC and The Barcelona Institute of Science and Technology, CIBER-BBN, Campus UAB, Bellaterra, Spain

[2] Instituto de Microelectrónica de Barcelona (IMB-CNM, CSIC), Campus UAB, Bellaterra, Spain

[3] Advanced NEMS Group, École Polytechnique Fédérale de Lausanne (EPFL), CH-1015 Lausanne, Switzerland

* Corresponding author: e-mail: mar.alvarez@imb-cnm.csic.es

Mechanically coupled resonators have been applied in the last years to the development of nanomechanical mass-sensors based on the detection of the different vibration modes of the system by measuring on a single resonator. Their sensitivity and capability for detecting multiple analytes strongly depends on the design and coupling strength between the mechanically coupled resonators in an array format. We present a theoretical and experimental study of the behavior of an asymmetrically coupled array of four different resonators. These doubly clamped beam resonators are elastically coupled by an overhang region of varying length along the transversal axis of the array. The results show that parameters such as the gap between microbeams and the overhang length affect the coupling strength, tuning the system from highly disordered and highly localized (weak coupling) to highly delocalized (strong coupling). In the strong coupling and partially-localized case, the distances between resonant peaks are larger, reaching higher eigenfrequency values. In this case, relative changes in a specific eigenstate, due to an added mass, can be markedly large due to the energy distribution over a single microbeam. A strong coupling also facilitates performing the detection on the relative frequency shift mode which can usually be resolved with better precision than the amplitude changes.

One of the key features sought when developing a mass sensor is the capability to simultaneously detect several analytes. In the case of microcantilevers or microbeams based biosensors, the development of a high-throughput system involves not only the fabrication of arrays of microcantilevers, which is currently a well-established and low-cost process, but also the implementation of a complex read-out system to independently read each microcantilever response.[1–3]

The use of mechanically coupled resonators arises as an alternative to avoid this drawback, by allowing the detection of several resonators using a single input and single output approach.[4,5] The mechanical coupling of an array of resonators to a common mass produces a mode localization phenomenon. An action on any of the resonators affects the vibration state of the other resonators. When adding a perturbation (e.g., a mass) to the coupled resonators, the periodicity of the system is broken, changing the dynamics of the structure and leading to the localization of the vibration energy at certain areas of the system (Anderson's localization).[6]

Coupled systems present several resonance peaks where each peak is related to a specific mode of the coupled system. The resonant peaks of the coupled system expand depending on the stiffness of the coupling region between resonators, k_c. For periodic, four identical mechanically coupled resonators, with identical stiffness k and effective mass m, the minimum resonance frequency corresponds to the an isolated oscillator, while the maximum resonance frequency increases with the strength of the coupling,[7] as shown in Eq.(1).

$$\omega_1 = \sqrt{k/m}$$
$$\omega_4 = \omega_1\sqrt{1+4\kappa} \quad (1)$$

where κ is the coupling coefficient, defined as the ratio of stiffness of the coupling element to the stiffness of the resonating element, $\kappa = k_c/k$. In the scope of this work, weak coupling is defined when $\kappa < 0.05$, while strong coupling is when $\kappa \geq 0.05$. When the coupled resonators are nearly identical, the eigenstates are said to be non-localized, and beautiful examples of collective dynamics can be found in the literature ,[8–11] and start becoming localized when a small mass is added to one of the resonators (in each eigenstate, one resonator oscillates more than the other).[12,13] By

decreasing the mechanical coupling coefficient, the relative changes between eigenstates (i.e., the normalized mode) can be larger than the relative change between the eigenvalues of a single resonator.[7,14] When such a strong localization occurs, the effect of the added mass causes a drastic change in the system dynamics,[15] enhancing the amplitude changes.[16,17] Working with an array of 15 nearly-identical coupled microcantilevers, Spletzer et *al.* propose the examination of experimentally measured patterns of eigenmode shifts to identify which microcantilever is detecting the analyte.[13] And Lee *et al.* demonstrate the feasibility of performing quantitative photoacoustic spectroscopy with six identical microcantilevers coupled to a shuttle mass.[18] However, although reducing the coupling would increase the responsivity in a weakly-coupled system, this would only work for small initial detuning of the individual frequencies. After some mass deposition, the system would lose the collective behavior and pass to be completely localized, being unusable for further sensing. Insertion of asymmetry or non-identical resonators in a coupled system provides a method with unique responses when any of the resonators is perturbed. In this way, DeMartini et *al.* demonstrate single input-single output multianalyte detection and identification, by measuring the resonance frequency variation of a coupled system that is strongly localized initially.[19,20] More recently, the signal-to-noise ratio amplification of strong coupled systems has been as well demonstrated.[21]

In this work, we make use of mechanically coupled resonators for implementing a system able to detect several analytes simultaneously, reducing the required read-out instrumentation and simplifying the data processing, while maintaining a high sensitivity and dynamic range. To that end, we propose an original geometry of four dissimilar frequency resonators with different (asymmetric) mechanical coupling between neighboring resonators to modulate the coupled system response. We investigate the effect of the coupling strength on the performance of such a system experimentally and numerically by using finite element analysis (FEA).

The proposed mechanical sensor is composed of an array of four microbeams clamped at both ends by an overhang region of varying length along the array. To achieve this, the set of microbeams is fabricated inside a trapezoidal frame, with a specific slope on two of the sides, as shown in Fig. 1 (a), which leads to microbeams with small variations in their lengths and, therefore, in their natural individual non-coupled resonance frequencies. At the same time, the coupling stiffness ratio, $\kappa = k_{c,i}/k_{b,i}$ (with $k_{c,i}$ being the coupling region spring constant and $k_{b,i}$ being the beam spring constant), is different between neighboring resonators, being lower for beams with smaller overhang length.[14] Different combinations of the frame slope, the gap between microbeams and the microbeam widths are analyzed. The proposed system can be considered initially disordered in the sense that all the resonators have different individual natural frequencies.

The mechanical sensor is fabricated following a process that is described in detail in the Supporting Material (Fig. S1). We fabricate various different arrays of four doubly clamped beam resonators into 300 μm length frames. We sweep three parameters in the design: slope angle of the coupling region (3°, 5° and 7°), beam width ($w = 10\ \mu m, 20\ \mu m$ and $35\ \mu m$) and inter-beam gap ($g = 10\ \mu m$ and $20\ \mu m$), for a total of 18 different designs. The thickness of the beams is 2 μm. Silicon nitride and silicon oxide are the microbeams main structural material. We achieve the coupling ledge, see Fig. 1(a) and 1(b), in silicon nitride by over-etching during release with Tetramethylammonium Hydroxide 25% (TMAH).

The characterization of these devices is performed using an in-house free-space optical interferometer, locating the laser spot approximately in the middle of each beam. The frequency spectra are obtained by performing a Fast Fourier Transform (FFT) of the thermomechanical noise response of the array. Using the Brownian motion of the devices ensures that the response of the system is spatially uncorrelated.[22] To simplify the analysis and discussion within this paper, all amplitudes are normalized to the maximum value that is obtained in each measurement. Fig. 1(c) shows the frequency spectra for an array configuration of four microbeams of 10 μm width, 10 μm gap and slope of 7°. The peaks in the spectra correspond to the first four eigenstates of the coupled system. As expected from theory,[23] the relative vibration amplitude of each mode depends on the geometry of the whole array but also on the beam on which the measurement is done.

Fig. 1. Image of the fabricated coupled array structure: (a) under the optical microscope and (b) under SEM. (c) Modal analysis of the first four eigenstates obtained by FEA, and experimental resonance spectra when focusing on the middle of each microbeam.

Finite element simulations of the system indicate that the lowest resonance peak in the frequency spectrum corresponds to an eigenstate where all the resonators move in-phase, see Fig. 1(c). The next three eigenstates of the structure correspond to the out-of-plane vibration modes where one of the microbeams moves out of phase.

The position of the individual modes within the coupled system strongly depends on the coupling coefficient, κ, which varies with the coupling region geometry. An increase in the length of the coupling region (i.e. higher slopes), facilitates the distribution of the energy in the coupled system, inducing a more delocalized response of the vibration modes (strong coupling). Consequently, the separation of the frequency peaks augments, facilitating the identification of each eigenstate. This is confirmed experimentally for systems of minimum beam width and gap (g=10 μm, w =10 μm), where the coupling between resonators increases for higher slopes (see Fig. S2 in the Supplementary Material). The system eigenfrequencies overlap for the case of a slope of 3° which presents a narrow frequency splitting (Δf=20 kHz) and the lower coupling coefficient estimated from Eq.(1) (κ= 0.015). The total splitting increases with the slope angle, attaining values of Δf=43 kHz for 5° and Δf=74 kHz for 7°. Increasing the slope angle and reducing the gap [14] provide the largest splitting (strongest coupling, κ> 0.05).

For a given slope, the coupling between resonators decreases when the gap of the microbeams increase, as shown in Fig. 2 for a slope of 7°. As expected, the response of arrays with narrower microbeams occurs at higher frequencies and with larger frequency splitting. Similarly, arrays with smaller inter-beam gaps show larger frequency splitting because of the stronger coupling.

Fig. 2. Effect of the microbeam width and gap on the minimum resonant frequency of the system (bars representing the frequency splitting, the distance between maximum and minimum frequency), for a frame slope of 7º.

Finite element modelling for different geometries reproduces the experimental behavior described in the previous paragraph (Fig. 3). When the slope of the ledge is the smallest, the coupling is also the smallest, and the system is disordered and weakly coupled, with the eigenstates localized in each individual beam for each vibration mode. In the case of an angle of 5°, only the first mode is totally localized, while the second, third and fourth eigenstates are non-localized. Finally, the system would be strongly coupled, with all the microbeams vibrating in all the system modes, for an angle of 7°, 10 μm width and 20 μm gap.

Fig. 3. Finite element modelling of the shape-mode for different array configurations (from weak-coupled and highly-localized, to strong-coupled and highly delocalized).

Depending on the strength of coupling and the magnitude of disorder, upon mass addition the vibration energy localizes more in certain beams of the structure. Adding a mass to one of the beams tends to localize more the vibration around the loaded beam at lower frequencies. If sufficient mass is added, the eigenstate with the lowest frequency corresponds to a vibration of the beam where the mass was added, and that alone.

In order to experimentally evaluate the effect of mass change over the system, we deposit a volume of a thermally killed bacteria (Listeria) solution 10 nM (in SSC 5x buffer) by using a drop deposition system able to print spots down to 10 μm (NanoEnabler system, Bioforce, USA). The printed volume is deposited at the middle of a beam (in the case shown in Fig 4(a), this is beam B4) to maximize the effect of the mass change with respect to that of the stiffness change (which is higher when the load is added near the clamped ends).[24] The volume is then dried before the measurement to stick it to the beam.

Fig 4(a) shows the largest frequency change (before/after mass addition) on the fourth eigenstate, which is consistent with the finite element modelling results. As expected, the observed frequency shift does not depend on the beam where we perform the measurement, other than a slight shift due to warming up of the beam.[25] The mass responsivity of the i[th] mode, is defined as $\Re \approx \Delta f_i/\Delta m_{eff}$, where m_{eff} is the mode effective mass.

Fig 4(a) also shows the change in vibration amplitude, i.e. change in the eigenmodes. In this case, we can evidently see a strong variation depending on the beam where we focus the laser spot. Zero amplitude change indicates that the

This manuscript was accepted by Appl. Phys. Lett. Click here to see the version of record.

amplitude of the mode does not change after adding the mass. It also shows that, while the effect of adding the mass is certainly measurable, it is different depending on the modes, and may even be opposite for certain modes in this strongly coupled asymmetric system (see also Fig. S3 in the Supplementary Material). This suggests that a detection method based on frequency shifts may be more adequate when using strongly coupled arrays,[26] as opposed to the mainstream thought of using amplitude measurements.[12]

Fig. 4. (a) Experimentally measured frequency and amplitude changes after adding a mass onto the B4 of a coupled array of microbeams with 10 µm width, gap of 10 µm and tilt angle of 5°. (b) Finite element simulations results for the same array configuration before and after adding a homogeneous mass of 75x10x1µm^3 on the center of the fourth beam.

Fig. 4(b) shows the results of finite element simulations when a mass that covers a whole central area of the B4 beam is added. The simulations show that the main effect of adding the mass is to concentrate the energy of the first mode on the microbeam being loaded, which agrees with the experimental observations, where the energy of the system is redistributed towards the first vibration mode when focusing on B4. Further simulations in which the load is applied to different beams confirm this point (see Fig. S4 in the Supplementary Material).

The dimensions, density and location of the added mass, as well as the pre-stress magnitude, are chosen in the simulation (within a realistic boundaries) to match the experimentally measured frequencies (see Table I). One possible cause of discrepancies between experimentally measured and simulated frequency values is the local variations in dimensions and properties (e.g. the simulations assumed homogeneous pre-stress for the whole array).

Table I. Comparison of the simulated, F_{sim}, and measured, F_{exp}, eigenvalues (kHz), before and after adding a mass.

	F exp.	F sim.	F mass exp.	F mass sim.
peak 1	699.08	711.45	695.89	693.04
peak 2	710.62	715.92	703.36	709.08
peak 3	723.03	721.32	715.71	714.32
peak 4	742.30	731.12	731.37	720.85

In conclusion, we discuss the interplay of different parameters on the coupling strength of different length asymmetrically coupled resonators. Various geometries are studied ranging from highly localized (weak coupling) to highly delocalized (strong coupling) systems. The results show the effect of the design on the final sensitivity of the system for mass sensing. With the proposed design, if sufficient mass is added into a beam, the eigenstate with the lowest frequency corresponds to a vibration of the beam where the mass is added. This makes it possible to identify the beam reacting during a biodetection by measuring the mode amplitude change. Also, a strong coupling facilitates performing the detection on the relative frequency shift mode which can usually be resolved with better precision than the amplitude changes.

Supplementary Material

Supplementary material containing detailed information about the fabrication process and additional graphs of the system behavior (experimental and simulated) is available.

The authors acknowledge the financial support from National Council for Science and Technology (CONACyT-Mexico); from the Ministerio de Economía y Competitividad (MINECO) (Spain) through Ramon y Cajal program (RYC-2013-14479) and MINAHE 5 MINECO/ICTI 2013-2016/ TEC2014-51940-C2 and by the EU ERDF (FEDER) funds; and from the Swiss National Science Foundation (PP00P2-144695). Fabrication of devices was done at the Spanish ICTS Network MICRONANOFABS partially supported by MINECO under project NGG-244 (GICSERV program). The authors also acknowledge C. Pascual-Izarra for the discussion and revision.

[1] A. Alodhayb, S.M.S. Rahman, S. Rahman, P.E. Georghiou, and L.Y. Beaulieu, Sens. Actuators B Chem. **237**, 459 (2016).
[2] N. Maloney, G. Lukacs, N. Nugaeva, W. Grange, J.P. Ramseyer, J. Jensen, and M. Hegner, J. Sens. **2012**, e405281 (2011).
[3] M. Alvarez and J. Tamayo, Sens. Actuators B **106**, 687 (2005).
[4] A.A. Glean, J.A. Judge, J.F. Vignola, and T.J. Ryan, J. Appl. Phys. **117**, 054505 (2015).
[5] S. Stassi, A. Chiadò, G. Calafiore, G. Palmara, S. Cabrini, and C. Ricciardi, Sci. Rep. **7**, 1065 (2017).
[6] P.W. Anderson, Phys. Rev. **109**, 1492 (1958).
[7] P. Thiruvenkatanathan, J. Woodhouse, J. Yan, and A.A. Seshia, J. Appl. Phys. **109**, 104903 (2011).
[8] Q. Chen, L. Huang, and Y.-C. Lai, Appl. Phys. Lett. **92**, 241914 (2008).
[9] R. Lifshitz and M.C. Cross, Phys. Rev. B **67**, 134302 (2003).
[10] R.B. Karabalin, M.C. Cross, and M.L. Roukes, Phys. Rev. B **79**, 165309 (2009).
[11] E. Kenig, M.C. Cross, R. Lifshitz, R.B. Karabalin, L.G. Villanueva, M.H. Matheny, and M.L. Roukes, Phys. Rev. Lett. **108**, 264102 (2012).
[12] M. Spletzer, A. Raman, A.Q. Wu, X. Xu, and R. Reifenberger, Appl. Phys. Lett. **88**, 254102 (2006).
[13] M. Spletzer, A. Raman, H. Sumali, and J.P. Sullivan, Appl. Phys. Lett. **92**, 114102 (2008).
[14] E. Gil-Santos, D. Ramos, V. Pini, M. Calleja, and J. Tamayo, Appl. Phys. Lett. **98**, 123108 (2011).
[15] C. Pierre and E.H. Dowell, J. Sound Vib. **114**, 549 (1987).
[16] D. Endo, H. Yabuno, K. Higashino, Y. Yamamoto, and S. Matsumoto, Appl. Phys. Lett. **106**, 223105 (2015).
[17] D.F. Wang, X. Li, X. Yang, T. Ikehara, and R. Maeda, J. Micromechanics Microengineering **25**, 095017 (2015).
[18] D. Lee, S. Kim, C.W.V. Neste, M. Lee, S. Jeon, and T. Thundat, Nanotechnology **25**, 035501 (2014).
[19] B.E. DeMartini, J.F. Rhoads, S.W. Shaw, and K.L. Turner, Sens Actuators A **137**, 147 (2007).
[20] B.E. DeMartini, J.F. Rhoads, M.A. Zielke, K.G. Owen, S.W. Shaw, and K.L. Turner, Appl. Phys. Lett. **93**, 054102 (2008).
[21] S. Ilyas, N. Jaber, and M.I. Younis, J. Microelectromechanical Syst. **25**, 916 (2016).
[22] E. Gil-Santos, D. Ramos, A. Jana, M. Calleja, A. Raman, and J. Tamayo, Nano Lett. **9**, 4122 (2009).
[23] R.B. Karabalin, *PhD Dissertation, Caltech* (2008).
[24] K. Zhang, Y. Chai, and J. Fu, AIP Adv. **5**, 127109 (2015).
[25] T. Larsen, S. Schmid, L.G. Villanueva, and A. Boisen, ACS Nano **7**, 6188 (2013).
[26] M.S. Hajhashemi, A. Rasouli, and B. Bahreyni, J. Microelectromechanical Syst. **25**, 52 (2016).

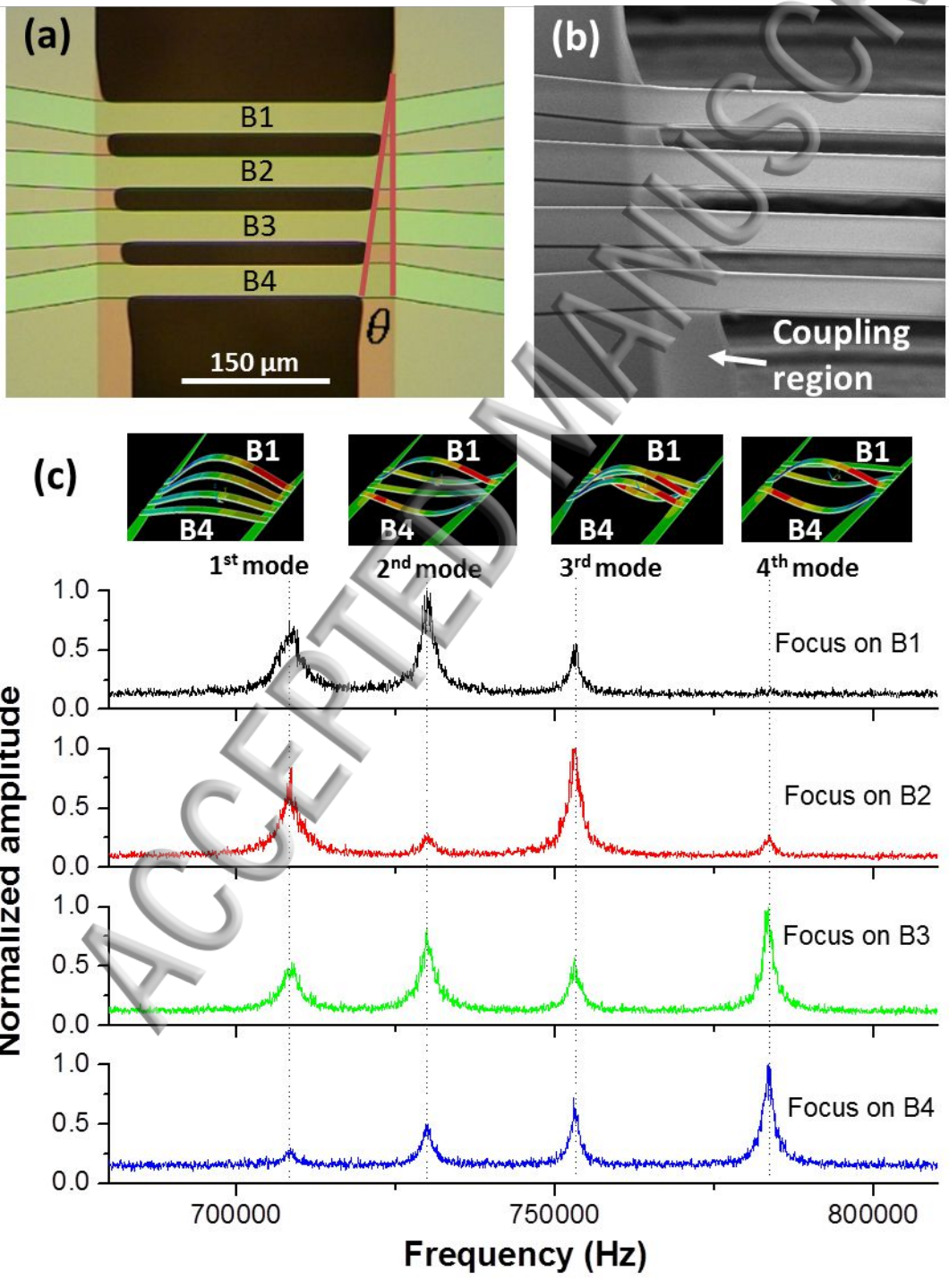

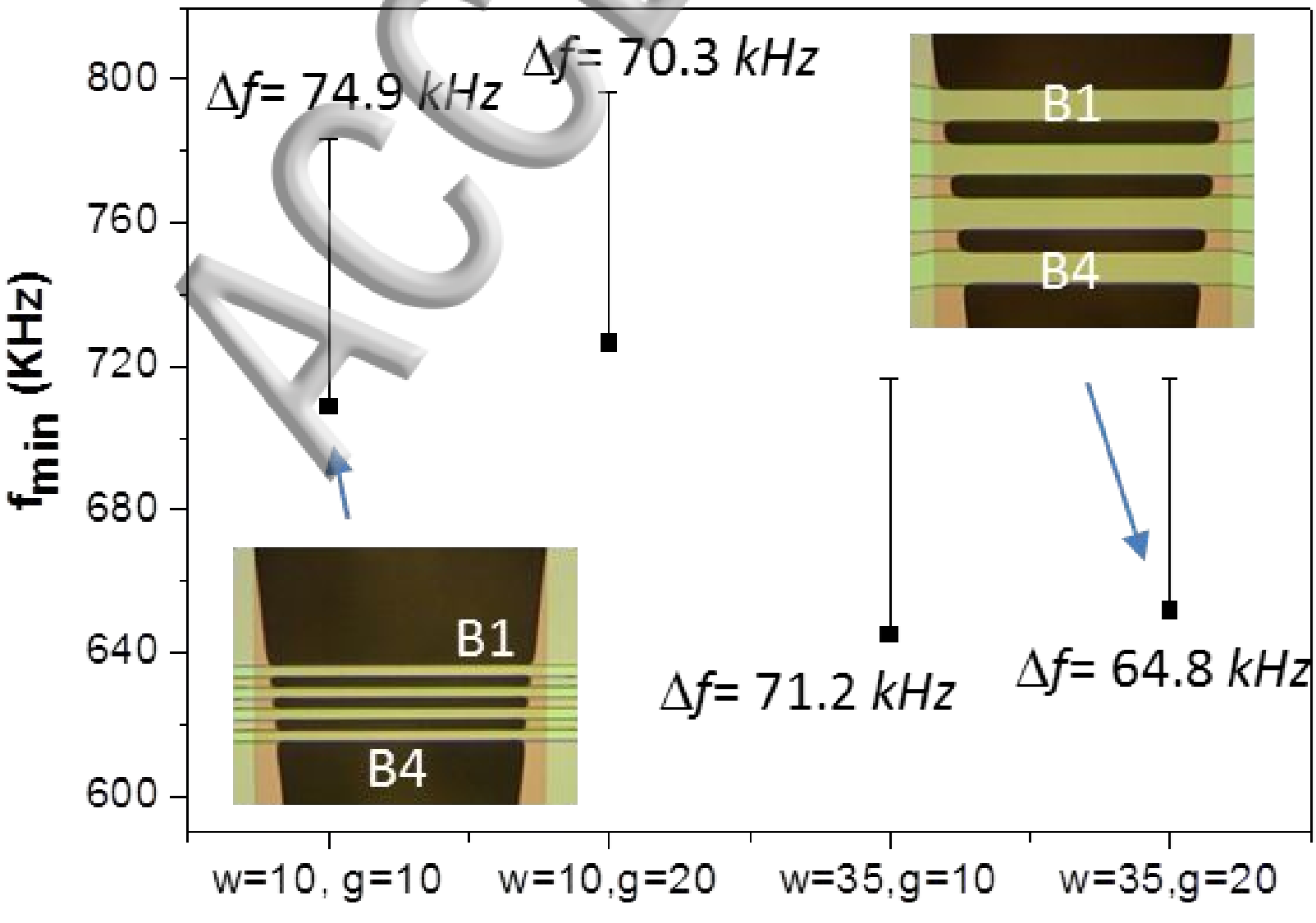
800
760
720
680
640
600
f_{min} (KHz)
Δf= 74.9 kHz
Δf= 70.3 kHz
Δf= 71.2 kHz
Δf= 64.8 kHz
B1
B4
B1
B4
w=10, g=10
w=10,g=20
w=35,g=10
w=35,g=20

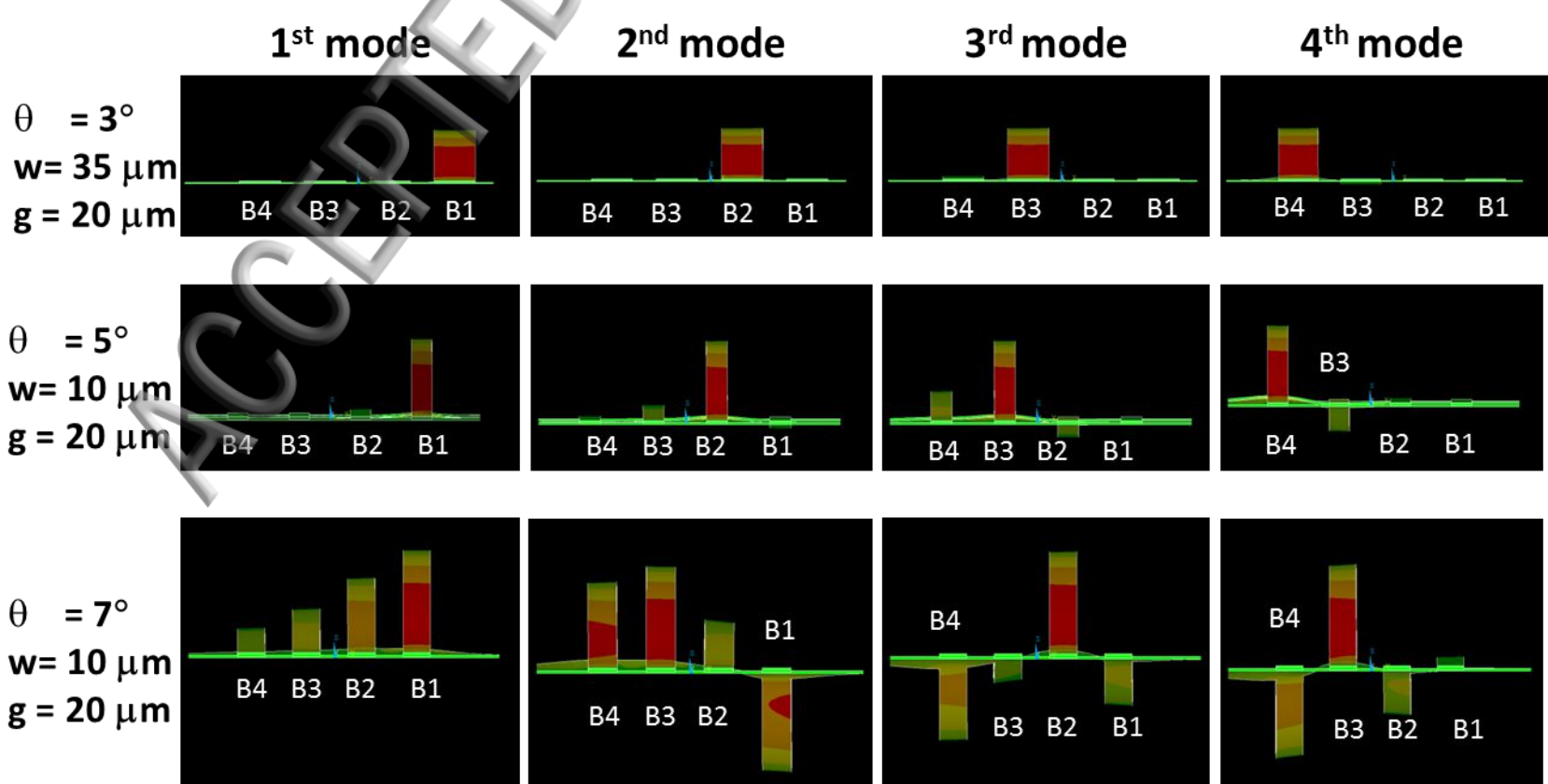
1st mode
2nd mode
3rd mode
4th mode
θ = 3°
w= 35 μm
g = 20 μm
θ = 5°
w= 10 μm
g = 20 μm
θ = 7°
w= 10 μm
g = 20 μm
B4 B3 B2 B1
B3
B1

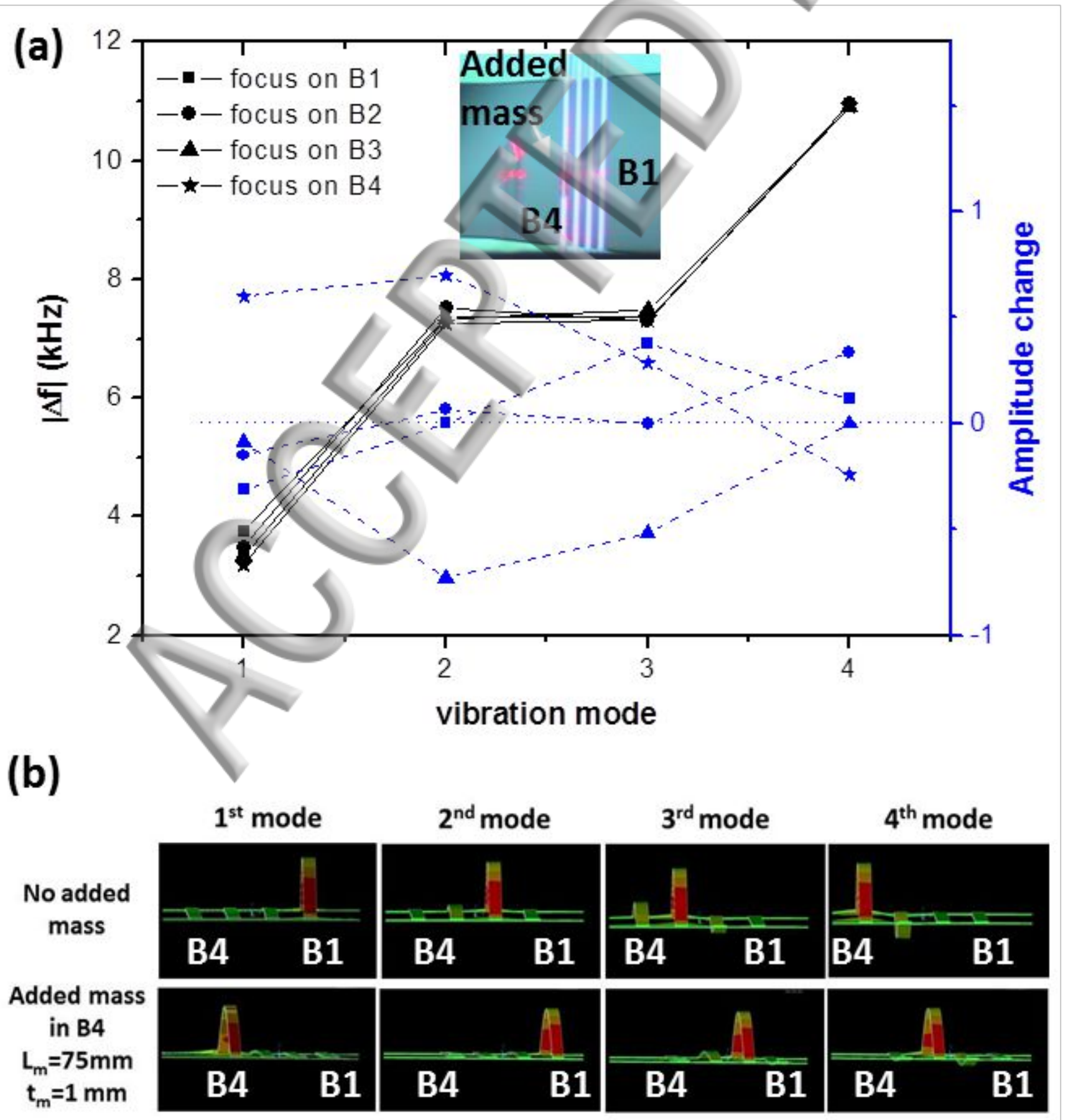
(a)
focus on B1
focus on B2
focus on B3
focus on B4
Added mass
B1
B4
|Δf| (kHz)
Amplitude change
vibration mode
(b)
1st mode
2nd mode
3rd mode
4th mode
No added mass
Added mass in B4
Lm=75mm
tm=1 mm
B4
B1